

## Silencing p53 inhibits interleukin 10-induced activated hepatic stellate cell senescence and fibrotic degradation in vivo

Qilan Guo<sup>1,2</sup> , Minghua Chen<sup>1</sup>, Qingduo Chen<sup>1</sup>, Guitao Xiao<sup>1</sup>, Zhixin Chen<sup>1</sup>, Xiaozhong Wang<sup>1</sup> and Yuehong Huang<sup>1,2</sup> 

<sup>1</sup>Department of Gastroenterology, Fujian Medical University Union Hospital, Fuzhou 350001, China; <sup>2</sup>Department of Geriatrics, Fujian Medical University Union Hospital, Fuzhou 350001, China

Corresponding author: Yuehong Huang. Email: 2003huangyh@sina.com; Xiaozhong Wang. Email: drwangxz@163.com

### Impact statement

This work further expanded the knowledge of the molecular mechanisms underlying IL-10 anti-fibrogenic effect by exploring the function of p53 in IL-10-induced activated HSCs senescence and fibrotic degradation *in vivo*. Our data showed that IL-10 gene intervention could lighten hepatic fibrosis induced by CCL<sub>4</sub> and induce the senescence of activated HSCs accompanied by up-regulating the expression of senescence-related proteins. In addition, depletion of p53 could abrogate up-regulation of IL-10 on the expression of aging-related proteins *in vivo* and *in vitro*. Moreover, p53 knockout in fibrotic mice could block the senescence of activated HSCs and the degradation of fibrosis induced by IL-10 gene treatment. In summary, our results suggested that IL-10 gene intervention could attenuate CCL<sub>4</sub>-induced hepatic fibrosis by inducing senescence of activated HSCs *in vivo*, and this induction was closely related to p53 signaling pathway. Our study sheds important light into the anti-fibrogenic therapy of IL-10.

### Abstract

Activated hepatic stellate cells are reported to play a significant role in liver fibrogenesis. Beside the phenotype reversion and apoptosis of activated hepatic stellate cells, the senescence of activated hepatic stellate cells limits liver fibrosis. Our previous researches have demonstrated that interleukin-10 could promote hepatic stellate cells senescence via p53 signaling pathway *in vitro*. However, the relationship between expression of p53 and senescence of activated hepatic stellate cells induced by interleukin-10 in fibrotic liver is unclear. The purpose of present study was to explore whether p53 plays a crucial role in the senescence of activated hepatic stellate cells and degradation of collagen mediated by interleukin-10. Hepatic fibrosis animal model was induced by carbon tetrachloride through intraperitoneal injection and transfection of interleukin-10 gene to liver was performed by hydrodynamic-based transfer system. Depletions of p53 *in vivo* and *in vitro* were carried out by adenovirus-based short hairpin RNA against p53. Regression of fibrosis was assessed by liver biopsy and collagen staining. Cellular senescence in the liver was observed by senescence-associated beta-galactosidase (SA- $\beta$ -Gal) staining. Immunohistochemistry, immunofluorescence double staining, and Western blot analysis were used to evaluate the senescent cell and senescence-related protein expression. Our data showed that interleukin-10 gene treatment could lighten hepatic fibrosis induced by carbon tetrachloride and induce the aging of activated hepatic stellate cells accompanied by up-regulating the expression of aging-related proteins. We further demonstrated that depletion of p53 could

abrogate up-regulation of interleukin-10 on the expression of senescence-related protein *in vivo* and *in vitro*. Moreover, p53 knockout in fibrotic mice could block not only the senescence of activated hepatic stellate cells, but also the degradation of fibrosis induced by interleukin-10 gene intervention. Taken together, our results suggested that interleukin-10 gene treatment could attenuate carbon tetrachloride-induced hepatic fibrosis by inducing senescence of activated hepatic stellate cells *in vivo*, and this induction was closely related to p53 signaling pathway.

**Keywords:** Interleukin 10, gene therapy, p53, hepatic stellate cells, senescence, liver fibrosis

**Experimental Biology and Medicine 2021; 246: 447–458. DOI: 10.1177/1535370220960391**

### Introduction

The hallmark of hepatic fibrosis is the massive accumulation of extracellular matrix (ECM), and activated hepatic

stellate cells (HSCs) are the principal cellular source of ECM. In addition to phenotypic reversion,<sup>1</sup> activity inhibition and clearance of activated HSCs were considered effective anti-fibrotic measures.<sup>2,3</sup> Recent studies have found

that inducing activated HSCs senescence contributes to mitigate liver fibrosis.<sup>4</sup> Senescent-activated HSCs could reduce the deposition of collagen fibers, promote the degradation of collagen fibers, and enhance immune surveillance, thereby attenuating liver fibrosis.<sup>5–8</sup> Therefore, promoting senescence of activated HSCs has therapeutic implication for hepatic fibrosis.

Cellular senescence is a relatively stable cell cycle arrest that is implicated in many age-related diseases including cancer.<sup>9</sup> Senescent cells are characterized by the increase of senescence-associated beta-galactosidase (SA- $\beta$ -Gal) activity, irreversible arrest of cell cycle, induction of senescence-related protein P53, P27, P21, and P16<sup>INK4a</sup>,<sup>10</sup> formation of senescence-associated heterochromatin foci (SAHF),<sup>11,12</sup> and upregulation of senescence-associated secretory phenotype (SASP).<sup>9</sup> Together with tumor suppressor p16<sup>INK4a</sup>, high mobility group A1 (HMGA1) proteins, a marker of cellular senescence, are able to promote SAHF generation and proliferative arrest, and also stabilize senescence through contributing to the inhibition of proliferation-associated genes.<sup>13</sup> In addition, HMGA1 proteins play an instrumental role in the proinflammatory SASP by upregulating nicotinamide phosphoribosyltransferase (NAMPT) through an enhancer element.<sup>14</sup> Interleukin-10 (IL-10) is a pleiotropic cytokine with anti-inflammatory and anti-fibrotic properties.<sup>15–17</sup> Our previous studies demonstrated that IL-10 could attenuate hepatic fibrosis induced by carbon tetrachloride (CCL<sub>4</sub>) and porcine serum in rats.<sup>18,19</sup> But the anti-fibrogenic mechanism of IL-10 was poorly understood. Recently, we found that IL-10 promoted primary rat HSCs senescence by up-regulating the expression of p53 and p21 *in vitro*.<sup>20</sup> Moreover, we demonstrated that induction of HSCs senescence by IL-10 may be associated with p53-mediated signaling pathway *in vitro*.<sup>21</sup> As p53 plays a vital role in the senescence of activated HSCs mediated by IL-10 and then affect the progression of fibrosis, we sought to determine whether p53 knockdown could affect the senescence of activated HSCs and degradation of fibrosis mediated by IL-10. This work will contribute to elucidate the anti-fibrogenic mechanism of IL-10 and may shed important light into the anti-fibrogenic therapy of IL-10.

## Materials and methods

### Reagents and antibodies

The reagents and kits were used in present research: Carbon tetrachloride (Tianjin Damao Chemical Reagent Factory, China), olive oil (Chengdu Kelong Chemical Reagent Factory, China), pcDNA3.1-IL-10 expression plasmid, pcDNA3.1 empty plasmid, recombinant adenovirus particle AD-Trp53-RNAi (68825–1,68826–1,68827–1), negative control virus CON098 (hU6-MCS-CMV-EGFP) were purchased from Shanghai Genechem Co., Ltd (Shanghai, China); Rat hypersensitive two-step immunohistochemistry detection reagent, phthalate tissue antigen repair solution (PH=6.0), DAB immunohistochemistry color development kit (ZSGB-BIO; Beijing, China); SA- $\beta$ -gal

staining kit (Beyotime Biotechnology, China); Sirius red staining kit (Beijing Solarbio Science & Technology Co., Ltd, China); fluorescent anti-quenching agent (Invitrogen, United States); Hyaluronic Acid Detection Kit (Zhengzhou Autobio Engineering Co., Ltd, China). Antibodies were used in these experiments: HMGA1, P53, P27 (Cell Signaling Technology Company, United States); P21 (109199) and  $\alpha$ -smooth muscle actin ( $\alpha$ -SMA) (ab32575) (Abcam Company, Hong Kong, China);  $\beta$ -actin (Sigma, United States), P16 (OriGene, Canada); goat resistance to mouse/rabbit IgG H&L (Alexa Fluor<sup>®</sup>488) (Abcam, United Kingdom), goat resistance to mouse/rabbit IgG H&L (Alexa Fluor<sup>®</sup>594) (Invitrogen, United States).

### Animals

All animal studies were approved by the Animal Care Committee of Fujian Medical University (Fuzhou, China) and experiments were conducted in compliance with the Guidelines on Animal Experiments at Fujian Medical University (Fuzhou, China). Sprague-Dawley male rats (12–16 week old) and ICR male mice (weight 18  $\pm$  2 g) were bought from Fujian Medical University Animal Experiment Center (Fuzhou, China) (Certificate No: SCXK (Min) 2016–0002). Animals were bred in a temperature (23  $\pm$  3°C), humidity (50–70%), and photoperiod (12-h light/dark cycle) controlled room and access to food and water ad libitum.

### Animal model and experimental protocols in rats

Rat fibrotic model was constructed according to the previous study.<sup>18</sup> Rats were randomly divided into control group (group N,  $n = 10$ ), fibrosis model group (group M,  $n = 10$ ), pcDNA3.1 empty plasmid group (group P,  $n = 10$ ), and pcDNA3.1-rIL-10 plasmid intervention group (group I,  $n = 10$ ). Rats in group M, P, and I were treated with 40% CCL<sub>4</sub> (v/v in olive oil) twice a week for eight weeks, while rats in group N were treated with olive oil only through intraperitoneal injection. From the fourth week, rats in group N and M were treated weekly with Ringer's solution, while those in group P and I were treated weekly with pcDNA3.1 and pcDNA3.1-rIL-10 plasmid through intravenous injection, respectively. The preparation and injection of plasmid DNA were as described previously.<sup>18</sup> By the end of the eighth week, all rats were sacrificed under anesthesia of 2% sodium pentobarbital at a dosage 45 mg/kg. A brief modeling process is described in Figure 1(a). Serums were collected and some liver tissues were fixed in 10% formalin and 4% paraformaldehyde solution for subsequent histological analysis, immunohistochemistry, and/or immunofluorescence double staining analysis. Partly liver tissues were stored in  $-70^{\circ}\text{C}$  for protein analysis.

### Animal model and experimental protocols in mice

Thirty ICR male mice were randomly divided into five groups ( $n = 6$ ), group control: no shRNA and CCL<sub>4</sub> treatment, group CCL<sub>4</sub>+Ad.Fc: fibrotic mice were

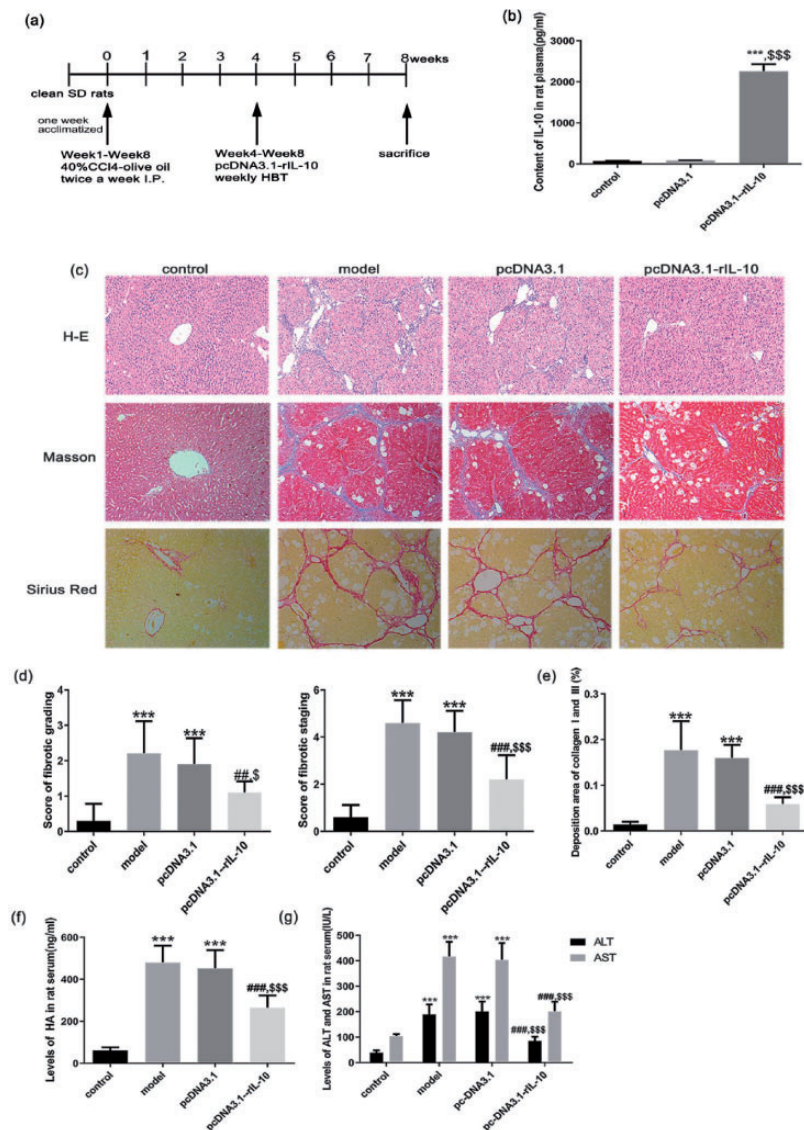


**Figure 1.** IL-10 gene intervention attenuated CCL<sub>4</sub>-induced hepatic fibrosis in rats. (a) Schematic diagram of drug intervention in the process of hepatic fibrosis induced by CCL<sub>4</sub> in rats. Liver fibrosis in SD male rats was induced by intraperitoneal injection of 40% (v/v) CCL<sub>4</sub>-olive oil mixed reagent, and pcDNA 3.1-rIL-10 recombinant plasmid and control reagent were injected through tail vein from the fourth week. (b) Content of IL-10 in rat plasma. After IL-10 gene intervention, the expression of IL-10 in rat plasma was significantly increased. (c) H&E (200 $\times$  magnification) and Masson stain (100 $\times$  magnification) were used to estimate the degree and grade of liver fibrosis; Sirius Red stain (100 $\times$  magnification) was used to observe deposition of collagen I and III. (d) Semi-quantitative analysis of grading of inflammatory and staging of fibrosis according to modified HAI score. (e) Expression of collagen I and III. (f) Serum level of HA. (g) Serum levels of ALT and AST.  $n = 10$ . Data were displayed as average  $\pm$  SD. \*\*\* $P < 0.001$ , compared with group control; ## $P < 0.01$ , ### $P < 0.001$ , compared with group model; \$ $P < 0.05$ , \$\$\$ $P < 0.001$ , compared with group pcDNA3.1. (A color version of this figure is available in the online journal.)

transfected with shRNA control via tail vein, group CCL<sub>4</sub>+Ad.Fc+IL-10: fibrotic mice were transfected with shRNA control and IL-10 gene, group CCL<sub>4</sub>+Ad.shp53+IL-10: fibrotic mice were transfected with target shp53 and IL-10 gene, group CCL<sub>4</sub>+Ad.shp53: fibrotic mice were transfected with target shp53 alone. CCL<sub>4</sub> was still used to induce the formation of liver fibrosis in mice. Adenoviruses bearing shRNA ( $2.5 \times 10^7$  pfu/g, once every two weeks) were injected into mice by tail vein,<sup>22</sup> and a mixture of CCL<sub>4</sub> (5 mL/kg) and olive oil (v/v 1:9) was intraperitoneally injected into mice. All mice were sacrificed under anesthesia of 2% sodium pentobarbital at a dosage 100 mg/kg at the end of the eight-week

experiments. A brief modeling process is described in Figure 4(a). In addition to collecting mouse liver tissue as described above, serums from each group of mice were also collected and stored at  $-70^\circ\text{C}$ .

### Liver histopathology assay

The left lobe liver tissues of each group were collected, fixed in 10% formalin solution, embedded in paraffin, and sectioned. Then sections were stained with hematoxylin and eosin (H&E) and Masson's trichrome stain following deparaffinization with xylene and rehydration with ethanol. The grading of inflammation and staging of

fibrosis in the fibrotic liver tissue were evaluated by two pathologists, according to modified HAI score.<sup>23</sup> Accumulation of collagen I and III was detected by Sirius Red stain and the area of collagen was quantified by using Image-Pro Plus software (version 6.0; Media Cybernetics, USA) as previously described.<sup>19</sup>

### Liver function assays

The content of aspartate aminotransferase (AST) and alanine aminotransferase (ALT) in serum of each group was measured by automatic biochemical analyzer in our clinical laboratory.

### Detection of serum hyaluronic acid

The serum level of hyaluronic acid (HA) was detected by following the instructions of HA test kit in the clinical laboratory of our institution.

### SA- $\beta$ -Gal and immunohistochemistry double staining

SA- $\beta$ -Gal and  $\alpha$ -SMA were considered to be a specific marker of cellular senescence<sup>24</sup> and HSCs activation, respectively. This experiment used single and double staining of SA- $\beta$ -Gal staining or/and immunohistochemistry of  $\alpha$ -SMA to observe the aging of activated HSCs in liver tissue. Briefly, the frozen sections of the liver tissue were fixed with staining fixative at room temperature for 15 min and washed with PBS. The washed sections were then stained overnight with staining solution (including X-Gal, prepared according to the instructions) at 37°C. Endogenous peroxidase was removed with 30 mL/L H<sub>2</sub>O<sub>2</sub>. The tissue sections above were incubated with  $\alpha$ -SMA primary antibodies (1:200, Boster Biological Technology) in a humidified chamber at 4°C for overnight. After incubation, the sections were stained with instant Polink-2 plus Polymer HRP Detection System (cat. no. PV-9001/PV-9002; ZSGB-BIO; OriGene Technologies) and then incubated in a buffer solution containing 3,3'-diaminobenzidine tetrahydrochloride (DAB) to generate a brown reaction product. The sections were also re-stained with hematoxylin staining solution (Beyotime Institute of Biotechnology) and followed by visualization under a phase contrast microscopy (magnification,  $\times 100$ ).

### Immunofluorescence double staining

$\alpha$ -SMA was used as a marker for activation of HSCs. In order to observe the expression of the target proteins P53 and HMGA1 in liver tissues, immunofluorescence double staining technique was used. In short, paraffin slices were baked, dewaxed with xylene, and dehydrated with gradient alcohol. Sections immersed in 0.01 M citrate buffer (pH 6.0) were placed in a microwave oven for antigen retrieval for 20 min. Then 0.2% TritonX-100 was added for permeation, 3% H<sub>2</sub>O<sub>2</sub> deionized water to inactivate endogenous peroxidase, and 10% goat/donkey serum (selected according to secondary antibody) was incubated at 37°C for 2 h to block non-specific antibodies, followed by incubation with mixture of anti-p53 (1:100, Cell Signaling Technology, United States)/HMGA1 (1:100, Abcam, United Kingdom)

and anti- $\alpha$ -SMA (1:300, Abcam, United Kingdom) primary antibodies at 4°C for overnight. The slices were washed with TBST for three times and then incubated with secondary antibody Alexa Fluor 488 (Abcam, United Kingdom) and Alexa Fluor 594 (Invitrogen, United States) at 37°C for 1 h followed by DAPI for another 15 min. The slices were observed using a TE-2000 Nikon Inverted fluorescence microscope.

### The preparation and storage of the recombinant adenovirus particle

There were three different types of p53-interfering adenovirus, recombinant adenovirus particle AD-Trp53-RNAi (68825-1, 68826-1, 68827-1), purchased from Shanghai Genechem Co., Ltd (Shanghai, China). They used the AdMax adenovirus packaging system established by Professor Frank L. Graham for adenovirus packaging. HEK293 cells were co-transfected with adenovirus shuttle plasmids carrying exogenous genes and auxiliary packaging plasmids carrying most of the adenovirus genome (E1/E3 deletion), using Cre-loxP (or FLP/frt) recombinase cleavage system. A non-replicating recombinant adenovirus carrying an exogenous gene can be produced. Finally, the adenovirus was amplified and purified, then stored at -70°C.

### Screening of p53 RNA-interfering adenovirus and cell intervention

The detailed cloning information of the recombinant adenovirus is provided in Supplemental Information and Figure 3(a). The immortality mouse hepatic stellate cell line (HSC-T25) with good growth status was divided into 6-well culture plates one day before virus infection. According to the MOI value of adenovirus in each group (Table 1), appropriate amount of RNAi adenovirus particles were added into groups designed for HSC-T25 infection experiment on the day of infection. After three days of infection, the expression of GFP was observed under fluorescence microscopy. Those with infection efficiency greater than 50% continued to be cultured. Cells were collected after five days of infection, and the expression of target gene mRNA and protein was tested by RT-PCR and Western blot to determine the interference effect of target and expression of downstream senescence-related proteins P21, P27, and HMGA1 after inhibition of p53 (see the operation process of RT-PCR and Western blot for details).

### Real-time polymerase chain reaction

Real-time PCR was performed according to the methods described in previous articles.<sup>20</sup> Briefly, total RNA was extracted from HSC-T25 cells by TRIzol reagent, reverse transcribed to cDNA, and amplified using the SYBR Green PCR Master Mix. The primer sequences were as follows: p53 forward, 5'-TGG AAG GAA ATT TGT ATC CCG A-3' and reverse, 5'-GTG GAT GGT GGT ATA CTC AGA G-3'; GAPDH forward, 5'-GGT TGT CTC CTG CGA CTT CA-3' and reverse, 5'-TGG TCC AGG GTT TCT TAC TCC-3'. All experiments were repeated three times. Finally, using

**Table 1.** MOI of adenovirus infection in each group

Group	Titer/concentration(FU/mL)	MOI
AD-Trp53-RNAi(68825-1)	4E+10	20
AD-Trp53-RNAi(68826-1)	3E+10	10
AD-Trp53-RNAi(68827-1)	2E+10	30
Control virus CON098	2E+11	10

GAPDH as internal reference, the difference of mRNA expression between groups was calculated by  $2^{-\Delta\Delta CT}$  method.

### Western blot assay

Western blot was exerted as described previously.<sup>20</sup> Briefly, proteins from liver tissue or HSC-T25 cells were extracted using the lysis buffer (RIPA:phosstop:cocktail:PMSF = 100:10:1:1, final concentration of PMSF was 1 mmol/L). After boiling the samples at 95°C for 5 min, the denatured protein samples were loaded with equal amount (30–50 µg) and separated by SDS-PAGE. Next, the protein was transferred to the polyvinylidene fluoride membranes by electrophoresis. The membranes were first blocked with 5% skimmed milk powder or BSA (diluted with TBST) and then were incubated at 4°C for overnight with primary antibodies against  $\alpha$ -SMA (1:400, Abcam, United Kingdom), P53 (1: 500, Cell Signaling Technology, United States), P21(1:500, Abcam, United Kingdom), P27 (1:500, Abcam, United Kingdom), HMGA-1(1:500, Abcam, United Kingdom), P16 (1:500, OriGene, Canada), and  $\beta$ -actin (1:10,000, Sigma, United States), respectively. After incubation, the membranes were washed with TBST for five times and then incubated for 1 h at RT with horseradish peroxidase-conjugated secondary antibodies (1:10,000). The membranes were washed with TBST for five times again, and visualized using an ECL detection system (Beyotime Biotechnology, China). The bands were quantified in grayscale using Image J software (NIH, United States). Typical bands are derived from three independent experiments.

### Statistical analysis

The results were expressed as the means  $\pm$  SD of at least three independent sets of experiments, and one-way ANOVA with the *post hoc* Dunnett's test was used to determine significance of difference. Values of  $P < 0.05$  or less were considered to be statistically significant. Statistical analyses were performed using SPSS 24.0 software.

## Results

### IL-10 gene intervention attenuated CCL<sub>4</sub>-induced hepatic fibrosis in rats

It has been reported that IL-10 could alleviate liver fibrosis,<sup>25,26</sup> but its molecular mechanism was poorly understood. Previous studies in our laboratory have shown that IL-10 gene intervention by hydrodynamic-based transfection (HBT) could alleviate hepatic fibrosis in rats induced by porcine serum by inhibiting the activation of HSCs.<sup>19</sup>

To further uncover the protection effects of IL-10 on liver injury and fibrogenesis and its possible mechanism, we used ELISA to determine the concentration of IL-10 in rat plasma first. We found that the concentration of IL-10 recombinant gene in plasma after tail vein injection was significantly increased compared to normal group (Figure 1(b)), which is consistent with previous studies.<sup>19</sup> Then we detected the liver histologic changes in CCL<sub>4</sub>-induced fibrotic liver after IL-10 gene treatment. H&E and Masson stains showed that IL-10 gene intervention by HBT markedly improved liver histology by ameliorating hepatocyte's steatosis and necrosis, inhibiting infiltration of inflammatory cells around portal vein, and reducing deposition of collagen fibers in the liver (Figure 1(c)). Compared to model group, the semi-quantitative evaluation of liver biopsy showed that both grading of inflammatory and staging of fibrosis in IL-10 intervention group were significantly declined (Figure 1(d)). To further assess the impact of IL-10 on hepatic fibrogenesis caused by CCL<sub>4</sub>, liver sections were stained with Sirius Red staining for collagen I and III, which are the major components of ECM. The results demonstrated that the accumulation of interstitial collagen I and III was significantly reduced after IL-10 gene intervention (Figure 1(c) and (e)). These data indicated that IL-10 gene intervention could promote the degradation of collagen and hamper the progression of fibrosis in rats with liver fibrosis. Hyaluronic acid (HA) is mainly derived from HSCs, and serum HA level is a quantitative index that can sensitively reflect the severity of liver damage and fibrosis. Measurement of serum HA further supported that collagen production was reduced by IL-10 treatment in rats with liver fibrosis (Figure 1(f)). Additional biochemical analyses of serum enzymes were performed to verify the hepatic protective effects of IL-10. Our data demonstrated that IL-10 gene intervention reduced levels of ALT and AST in serum of CCL<sub>4</sub>-treated rats (Figure 1(g)). Together, these results confirmed that IL-10 gene intervention was able to alleviate CCL<sub>4</sub>-induced liver fibrosis in rats via inhibiting hepatic inflammatory and promoting degradation of collagen.

### IL-10-induced senescence of activated HSCs was associated with elevated p53 expression in vivo

Activated HSCs are the chief cellular source of ECM, and promoting the senescence of activated HSCs can reduce the degree of liver fibrosis caused by chronic liver injury.<sup>27</sup> Our previous study has confirmed that IL-10 could promote primary rat HSCs senescence by up-regulating senescence-associated protein P53 and its downstream protein P21 expression *in vitro*.<sup>20</sup> In the present study, we sought to further investigate whether the anti-fibrogenic effect of IL-10 was associated with the senescence of activated HSCs *in vivo*. Immunohistochemistry staining (IHC) and SA- $\beta$ -gal staining were used to detect the expression of  $\alpha$ -SMA (marker of activated HSCs) *in situ* and the senescence of activated HSCs in liver tissues, respectively. Firstly, IHC results indicated that numbers of  $\alpha$ -SMA-positive cells in group IL-10 treatment were significantly decreased compared with the group model and empty plasmid control

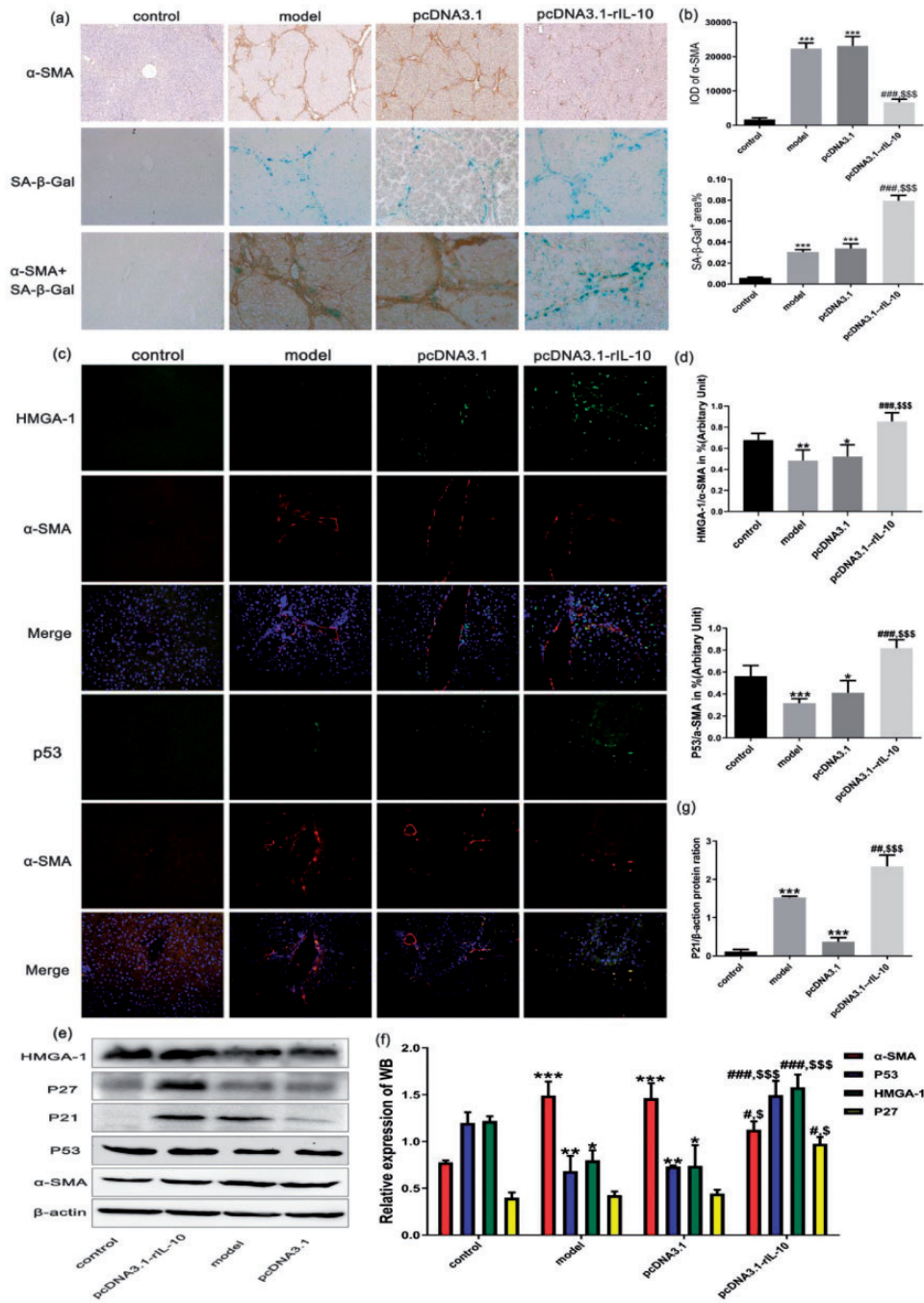


**Figure 2.** IL-10-induced senescence of activated HSCs was associated with increased expression of p53 *in vivo*. (a) Immunohistochemistry staining of  $\alpha$ -SMA and SA- $\beta$ -Gal staining was used to detect the numbers of activated HSCs and senescent HSCs in rats, respectively (100 $\times$  magnification). (b) Relative area of positive expression of  $\alpha$ -SMA or SA- $\beta$ -Gal (%) in liver tissue. (c) Immunofluorescence double staining to observe the expression of HMGA1 or p53 in fibrotic liver tissue. HSCs were specifically stained with antibody against  $\alpha$ -SMA, and nuclei were stained with DAPI (100 $\times$  magnification). (d) Bar graphs showed the percentage quantitation of fluorescent images of HMGA1 or P53 positive cells in all activated HSCs ( $\alpha$ -SMA as marker). (e, f, g) Western blot analyzed the expression levels of  $\alpha$ -SMA, P53, P21, P27, HMGA1 in liver tissue.  $n = 10$ . Data were displayed as average  $\pm$  SD. \* $P < 0.05$ , \*\* $P < 0.01$ , \*\*\* $P < 0.001$ , compared with group control; # $P < 0.05$ , ## $P < 0.01$ , ### $P < 0.001$ , compared with group model;  $^{\S}P < 0.05$ ,  $^{\S\S}P < 0.001$ , compared with group pcDNA3.1. (A color version of this figure is available in the online journal.)

(Figure 2(a) and (b)), which are similar to previous study.<sup>19</sup> These results suggested that IL-10 gene treatment has ability to inhibit the activation of HSCs or promote the clearance of activated HSCs. It is well known that senescent HSCs could enhance immune surveillance and then promote the clearance of senescent cells.<sup>3</sup> Next, we sought to clarify the relationship between anti-fibrotic effect of IL-10

and senescence of activated HSCs. The activity of SA- $\beta$ -gal, a marker of cellular senescence, was detected in fibrotic liver tissues after treatment with IL-10 gene. As illustrated in Figure 2(a), positive stain of SA- $\beta$ -gal activity was accumulated in fibrotic liver and mainly located along fibrous septa. Compared to other groups, the areas of SA- $\beta$ -gal positive stain in IL-10 treatment group were dramatically

increased (Figure 2(b)), suggesting that IL-10 gene treatment is able to increase SA- $\beta$ -gal activity in fibrotic liver. Thirdly, we sought to further investigate whether activated HSCs were the main cells of SA- $\beta$ -gal positive cells. The SA- $\beta$ -gal and  $\alpha$ -SMA immunohistochemistry double staining demonstrated that most areas of SA- $\beta$ -gal positive were also the  $\alpha$ -SMA-positive cells (Figure 2(a)). HMGA1, another senescence marker, was used to judge the cellular senescence in the tissue. HMGA1 and  $\alpha$ -SMA immunofluorescence double staining showed that expression of HMGA1 positive stain was co-localized with  $\alpha$ -SMA (Figure 2(c)). In addition, the expression of HMGA1 was increased in IL-10 gene treatment group compared with those in group model and pcDNA3.1 (Figure 2(d)). Together, these results indicated that IL-10 gene intervention could increase the numbers of senescent cells in rat fibrotic liver induced by CCL<sub>4</sub> and most senescent cells were activated HSCs.

As an important tumor suppressor gene, p53 plays a crucial role in cellular senescence in response to a series of cellular injury.<sup>22</sup> Our previous *in vitro* study has showed that IL-10 induced activated HSCs senescence via STAT3-p53 signaling pathway. To confirm whether p53 plays a vital role in senescence of activated HSCs induced by IL-10 in fibrotic liver, we examined the expression of p53 in rat fibrotic liver with different methods. Immunofluorescence double staining showed that expression of p53 in fibrotic liver was mainly in activated HSCs (Figure 2(c)). In addition, chronic CCL<sub>4</sub> intoxication could reduce the expression of p53 and IL-10 gene treatment has the opposite effect on its expression (Figure 2(d)). Western blot analysis further confirmed that senescence-associated proteins P53 and HMGA1 and their downstream target proteins P21 and P27 in liver tissue were markedly increased in IL-10 gene treatment group compared to group model and pcDNA3.1 (Figure 2(e) to (g)), suggesting that IL-10 gene treatment can promote the expression of senescence-related proteins and its downstream target proteins. Taken together, these results displayed that IL-10 gene treatment induced the senescence of activated HSCs *in vivo* accompanied with increased senescence-related protein P53 and its downstream target proteins.

#### Depletion of p53 abrogated the up-regulation effect of IL-10 on senescence-related proteins in HSC-T25 cells *in vitro*

To further investigate the role of p53 in senescence of activated HSCs induced by IL-10, short hairpin RNA (shRNA) technology, which leads to the knockdown of messenger RNA (mRNA) and protein, was used to deplete the p53 gene. Recombinant adenoviral particles encoding mouse p53 shRNA (AD-Trp53-RNAi) were used to deplete the expression of p53 mRNA and protein in cultured immortality mouse HSC-T25 cells (Supplemental Information and Figure 3(a)). The AD-Trp53-RNAi and negative control virus CON098 (hU6-MCS-CMV-EGFP) were used to transfect HSC-T25 cells treated with or without IL-10. When the infection rate was observed to be over 80% under the fluorescence microscope (Figure 3(b)), real-time PCR and

Western blot were used to identify the efficiency of p53 knockdown. Our results showed that p53-targeting shRNA induced not only significant and specific mRNA knockdown (the knockdown efficiency at the RNA level was greater than 70% in all three groups) but also protein knockdown (Figure 3(c) and (d)). Among them, Trp53-RNAi (68825-1) had the best inhibitory effect on p53 compared with other adenovirus groups, which was used to inhibit p53 expression in subsequent animal experiments. We also detected the expression of senescence marker protein HMGA1 and p53 downstream target proteins P21 and P27 in HSC-T25 cells after p53 knockdown. Our results indicated that the expression of HMGA1, P21, and P27 in HSC-T25 cells was significantly decreased in Ad.shp53 pretreatment compared to IL-10 treatment alone (Figure 3(d) and (e)). These data demonstrated that p53 knockdown by p53 shRNA alleviated the pro-senescence effects of IL-10 *in vitro*. Moreover, these results could provide an experimental foundation for subsequent animal experiments.

#### Depletion of p53 abrogated the anti-fibrotic effect of IL-10 on hepatic fibrosis in mice

To determine whether the anti-fibrogenic effect of IL-10 was associated with p53-mediated senescence of activated HSCs *in vivo*, recombinant adenoviral particles encoding mouse p53 shRNA (AD-Trp53-RNAi) with or without IL-10 gene were transferred into fibrotic liver by tail vein injection. Both histopathological and biochemical examinations were performed to assess the degree of liver fibrosis. H&E, Masson, and Sirius Red staining results stated that the liver inflammatory and fibrogenesis were decreased by IL-10 gene treatment alone compared with CCL<sub>4</sub> model group, which is consistent with the above results (Figure 1(d)), while depletion of p53 blocked the effect of IL-10 on liver inflammatory and degradation of ECM (Figure 4(b) to (d)). We next detected the levels of ALT and AST to assess the protective effect of IL-10 gene treatment. Our results stated that IL-10 gene intervention could reduce the levels of ALT and AST in fibrotic mice. In addition, the levels of ALT and AST were markedly increased in depletion of p53 group compared with IL-10 gene treatment alone (Figure 4(e)). These results indicated that p53 played a crucial role in the protective effect of IL-10 on liver injury. Moreover, we detected the levels of HA in serum to investigate the degradation of fibrosis. As shown in Figure 4(f), IL-10 gene treatment was able to reduce the levels of HA in fibrotic mice, which is similar to results in rat fibrotic model, and the levels of HA were markedly increased in depletion of p53 group compared with IL-10 gene treatment alone. Taken together, these findings demonstrated that depletion of p53 by p53 shRNA weakened the anti-fibrosis effect of IL-10 *in vivo*.

#### Depletion of p53 attenuated activated HSCs senescence mediated by IL-10 in mice

We next explored whether p53 was directly involved in the IL-10-induced HSCs senescence *in vivo*. The staining results of IHC and SA- $\beta$ -Gal in liver tissue of fibrotic mice were similar to those of rats after IL-10 gene intervention.

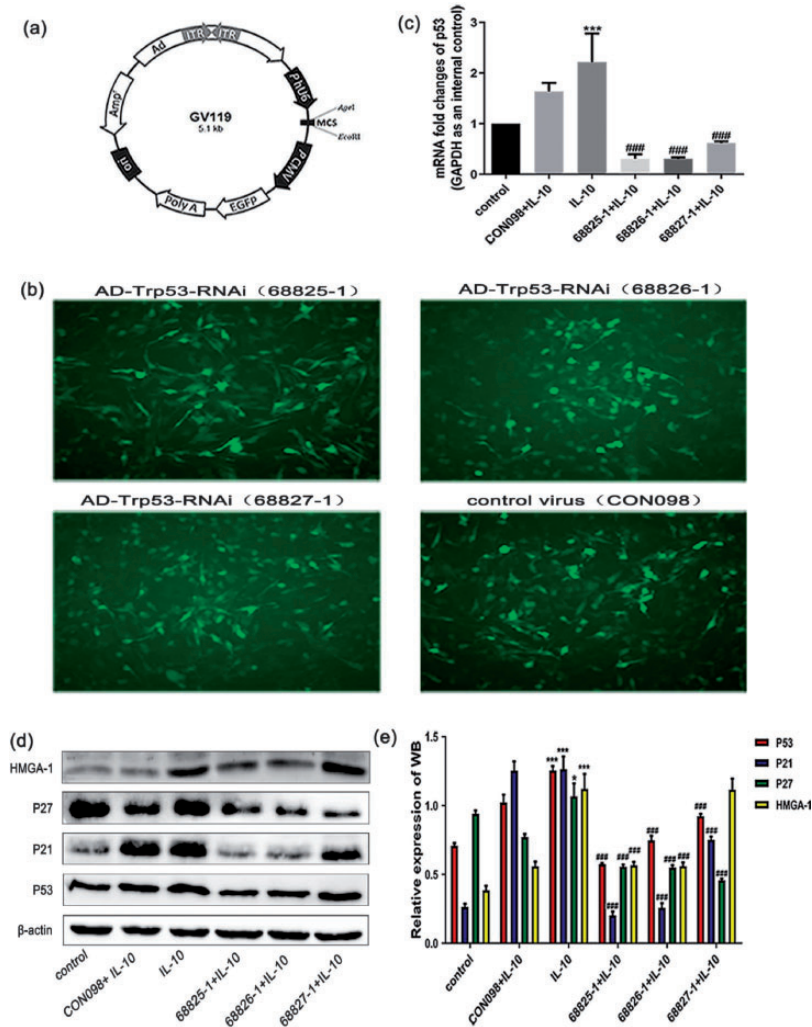


**Figure 3.** Inhibition of p53 antagonized IL-10-induced expression of senescence-related proteins in HSC-T25 cells *in vitro*. (a) Vector structure of recombinant adenovirus. (b) Performance of GFP in HSC-T25 cells under fluorescence microscopy after adenovirus transfection for three days (200 $\times$  magnification). The infection rate in all groups was above 80%. (c) Real-time PCR analyzed the mRNA expression of p53 after silencing p53. The knockdown efficiency at the RNA level was greater than 70% in all three groups. (d, e) Western blot analyzed the expression levels of p53 and its downstream target proteins P21, P27, and HMGA-1 after silencing p53. Data were displayed as average  $\pm$  SD. \* $P < 0.05$ , \*\*\* $P < 0.001$ , compared with group control; ### $P < 0.001$ , compared with group IL-10 intervention. (A color version of this figure is available in the online journal.)

However, after the recombinant adenovirus granule AD-Trp53-RNAi was transferred into fibrotic mice to block the expression of p53, the numbers of SA- $\beta$ -gal positive cells, which located along fibrous septa, were decreased and the numbers of  $\alpha$ -SMA positive cells were markedly increase compared to IL-10 gene treatment alone (Figure 5 (a) and (b)). These results indicated that depletion of p53 could inhibit the cellular senescence induced by IL-10 treatment. The immunofluorescence double staining of p53 or HMGA1 together with  $\alpha$ -SMA showed that the induction of IL-10 on activated HSCs senescence was weakened after depletion of p53 in fibrotic liver (Figure 5(c) and (d)). Moreover, Western blot were carried out to measure the expressions of senescence-related proteins P53, P21, P16, and P27, respectively. As expected, IL-10 gene treatment promoted the expression of aging-related proteins in fibrotic mice liver, and these effects were partially reversed by depletion of p53 (Figure 5(e) and (f)). In summary, these

data demonstrated that IL-10 induced activated HSCs senescence in a p53-dependent manner *in vivo*.

## Discussion

Liver fibrosis is an inevitable stage for most chronic liver diseases to progress to cirrhosis. Advanced cirrhosis can lead to severe complications such as massive hemorrhage of digestive tract, primary liver cancer, and liver failure, with high mortality rate and serious threat to human health.<sup>28</sup> However, there is still a lack of safe and effective drugs for the treatment of liver fibrosis. Therefore, it is of great significance to study the pathogenesis of liver fibrosis and find safe and effective drugs for the treatment of liver fibrosis.

IL-10 is a pleiotropic cytokine and has anti-inflammatory and anti-fibrotic activities.<sup>15–17</sup> Our previous studies have demonstrated that IL-10 gene intervention by HBT could

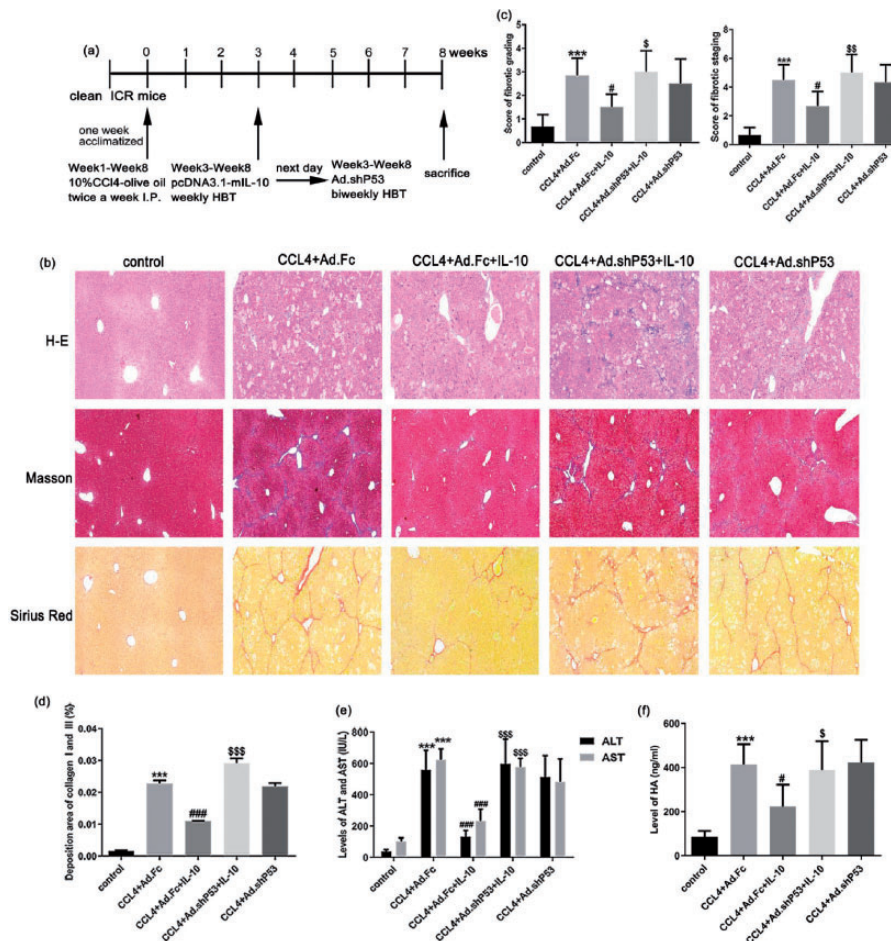


**Figure 4.** Depletion of p53 abrogated the anti-fibrotic effect of IL-10 on hepatic fibrosis in mice. (a) Schematic diagram of drug intervention in the process of hepatic fibrosis induced by CCL<sub>4</sub> in mice. Liver fibrosis in ICR male mice was induced by 10% (v/v) CCL<sub>4</sub>-olive oil mixed reagent. From the third week, pcDNA3.1-mIL-10 recombinant plasmid and empty plasmid were injected into mice by tail vein, and adenovirus inhibiting p53 and control virus were injected through tail vein the next day. (b) H&E and Masson stain were used to assess the degree and grade of liver fibrosis, Sirius Red stain was used to detect accumulation of collagen I and III (100× magnification). (c) Semi-quantitative analysis of grading of inflammatory and staging of fibrosis according to modified HAI score. (d) Expression of collagen I and III. (e) Serum levels of ALT and AST. (f) Serum levels of HA.  $n = 6$ . Data were displayed as average  $\pm$  SD. \*\*\* $P < 0.001$ , compared with group control; # $P < 0.05$ , ## $P < 0.01$ , ### $P < 0.001$ , compared with group CCL<sub>4</sub>+Ad.Fc; \$ $P < 0.05$ , \$\$\$ $P < 0.001$ , compared with group CCL<sub>4</sub>+Ad.Fc+IL-10. (A color version of this figure is available in the online journal.)

attenuate hepatic fibrosis induced by CCL<sub>4</sub> and porcine serum in rats.<sup>18,19</sup> HBT, an efficient method for transfecting plasmid DNA into hepatocytes *in vivo*, could achieve persistent and high levels expression of IL-10 in the liver. Therefore, HBT was applied to transfer IL-10 gene to liver in present study. The histologic and liver function test showed that IL-10 gene intervention promoted degradation of ECM, alleviated the liver injuries, and reduced the number of activated HSCs, which are similar to previous study.<sup>18,19</sup> Beside the phenotype reversion, both apoptosis and senescence of activated HSCs could reduce the number of activated HSCs.<sup>1-4</sup> Moreover, previous study has confirmed that IL-10 could promote HSCs senescence *in vitro*.<sup>20</sup> However, it is still unknown whether the anti-fibrogenic effects of IL-10 were associated with activated HSCs senescence *in vivo*. Immunofluorescence double staining was applied to detect whether the main senescent cells was the activated HSCs. HMGA1 (a marker of cellular senescence) and  $\alpha$ -SMA (a marker of activated HSCs) double staining results showed that the area of HMGA1

positive cell was similar to the area of  $\alpha$ -SMA. In addition, the HMGA1 and  $\alpha$ -SMA double positive cells were markedly increased in IL-10 gene treatment rats, suggesting that mostly senescent cells were the activated HSCs. These results were consistent with those of Jin *et al.*<sup>29</sup> Taken together, these findings showed that the anti-fibrogenic effect of IL-10 might be related to its induction of activated HSCs senescence *in vivo*.

Increasing studies showed that p53 plays a critical role in induction of activated HSCs senescence.<sup>20,29-31</sup> For example, curcumin could promote activated HSCs senescence accompanied by increased expression of p53, which suggested that p53 could be a therapeutic target for reducing HSCs activation.<sup>28</sup> In our study, p53 and  $\alpha$ -SMA double staining were used to judge whether IL-10-induced activated HSCs senescence was mediated by p53 *in vivo*. Our results showed that positive area and expression level of p53 were similar to HMGA1, suggesting that IL-10 gene intervention could promote expression of p53 in the senescent HSCs. Western blot analysis also confirmed that

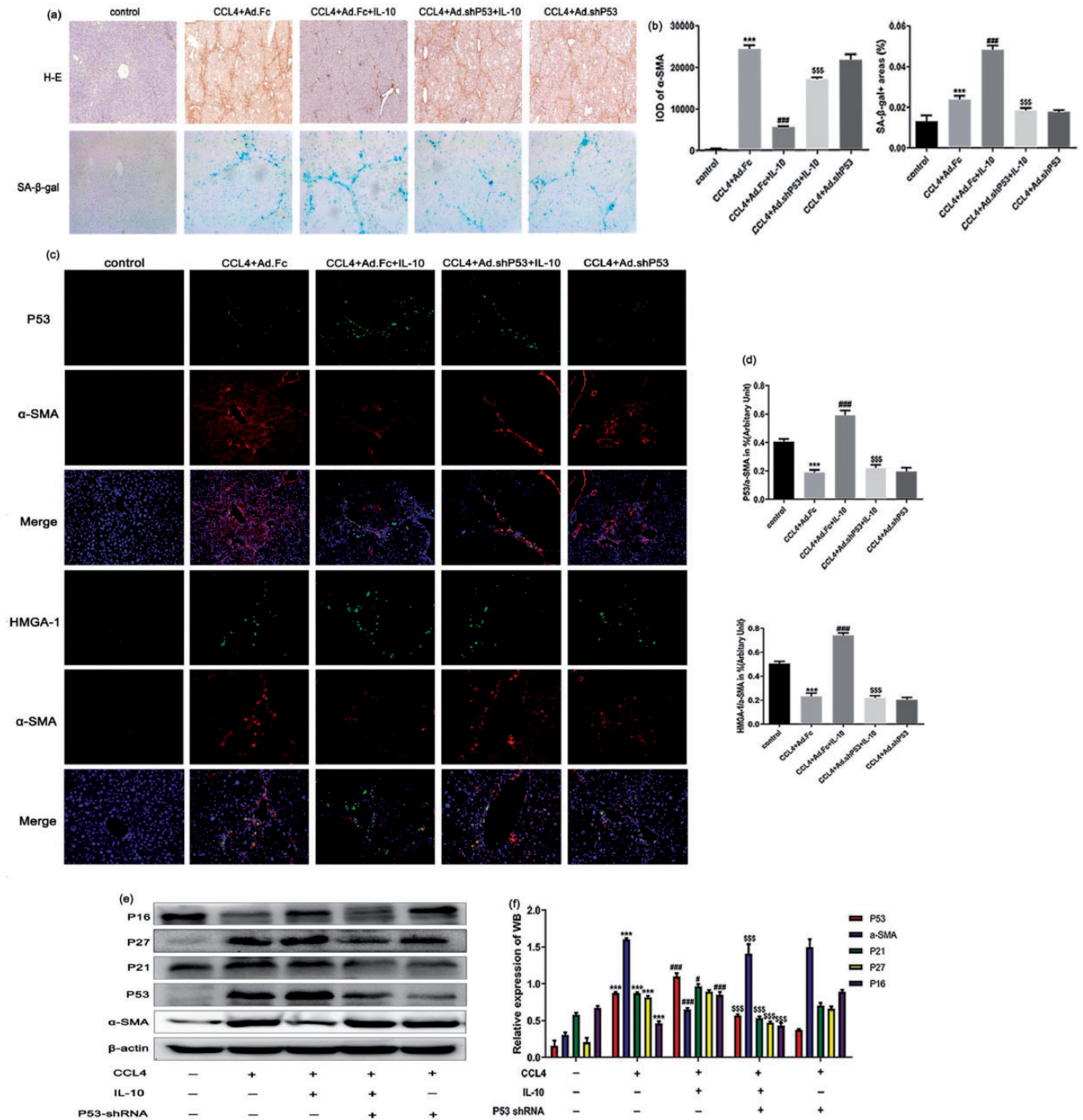


**Figure 5.** Depletion of p53 attenuated IL-10-induced activated HSCs senescence *in vivo*. (a) Immunohistochemistry staining of  $\alpha$ -SMA and SA- $\beta$ -Gal staining was used to detect the numbers of activated HSCs and senescent HSCs in mice, respectively (100 $\times$  magnification). (b) Relative expression of  $\alpha$ -SMA or SA- $\beta$ -Gal (%) in mice liver tissue. (c) Immunofluorescence double staining to observe the expression of p53 (200 $\times$  magnification) or HMGA1 (100 $\times$  magnification) in mice liver tissue. HSCs were specifically stained with antibody against  $\alpha$ -SMA, and nuclei were stained with DAPI. (d) Bar graphs showed the percentage quantitation of fluorescent images of P53 or HMGA1 positive cells in all activated HSCs ( $\alpha$ -SMA as marker). (e, f) Western blot analyzed the expression levels of  $\alpha$ -SMA, P21, P27, and P16 in mice fibrotic liver.  $n = 6$ . Data were displayed as average  $\pm$  SD. \*\*\* $P < 0.001$ , compared with group control; # $P < 0.05$ , ### $P < 0.001$ , compared with group CCL4+Ad.Fc; \$\$\$ $P < 0.001$ , compared with group CCL4+Ad.Fc+IL-10. (A color version of this figure is available in the online journal.)

expression levels of senescence-associated proteins HMGA1, P53, and its downstream target protein P21, P27 were significantly increased in IL-10 gene treatment rats compared with fibrotic model control rats. Thus, our data suggested that IL-10-induced senescence of activated HSCs was also associated with increased expression of p53 *in vivo*.

RNA interference (RNAi) is a natural process in which double-stranded RNA inhibits expression of a certain target protein by stimulating the specific degradation of the target gene mRNA. It is an useful method *in vitro* and *in vivo* to disrupt excessive expression of gene and to uncover the function of genes.<sup>32</sup> To further confirm that p53 played a key role in IL-10-induced activated HSCs

senescence, RNAi technology was used to deplete the expression of p53 in immortality mouse HSC-T25 cells *in vitro*. Our results showed that p53 gene could be effectively depleted and the expression of p53 and its downstream proteins was also significantly decreased. We next investigated the influence of p53 depletion on degradation of fibrosis and senescence of activated HSCs mediated by IL-10 in mice. Liver biopsy results showed that collagen deposition and inflammatory cells infiltration were markedly improved in IL-10 gene treatment group compared with those in shRNA control group. However, the anti-fibrotic of IL-10 is abrogated in p53 depletion group. The levels of AST, ALT, and HA in serum were decreased after IL-10 treatment but the results were conversed after p53 depletion. These data indicated that p53 depletion could block anti-fibrotic effect of IL-10 on degradation of fibrosis. As our results suggested that p53 played a crucial role in progression of liver fibrosis, we next evaluated whether p53 depletion affects the senescence of activated HSCs induced by IL-10 *in vivo*. IHC results showed that p53 depletion could reverse the effect of IL-10 on inhibition of  $\alpha$ -SMA. SA- $\beta$ -Gal staining showed that the number of senescent cells in p53 knockdown mice was markedly decreased compared to IL-10 treatment mice. These data indicated that p53 depletion could reverse promotion effect of IL-10 on cellular senescence. Immunofluorescence double stain result is similar to IHC. Western Blot results further demonstrated that the decreased expression of p53 and its downstream aging-related proteins P21, P27, and P16 in p53 depletion group compared with IL-10 gene treatment group. Together, these results suggested that p53 played an important role in senescence of activated HSCs mediated by IL-10. Silencing the expression of p53 is able to antagonize the senescence of activated HSCs induced by IL-10.

In conclusion, IL-10 gene treatment could induce activated HSCs senescence *in vivo* by up-regulating the expression of p53 and its downstream target proteins, thereby reducing the degree of CCL<sub>4</sub>-induced liver fibrosis. Depletion of p53 could abrogate the effect of IL-10 through promoting senescence of activated HSCs and degradation of fibrosis. This study provided a new perspective and theoretical basis for the clinical application of IL-10 in anti-fibrogenic therapy.

**Authors' contributions:** HYH and WXZ conceived the research ideas and supervised the project; GQL, CMH, CQD, and XGT carried out experiments, GQL and CZX analyzed the data. GQL wrote the manuscript, HYH revised the manuscript. All authors approved the final manuscript.

#### DECLARATION OF CONFLICTING INTERESTS

The author(s) declared no potential conflicts of interest with respect to the research, authorship, and/or publication of this article.

#### FUNDING

The author(s) disclosed receipt of the following financial support for the research, authorship, and/or publication of this

article: This work was supported by the National Natural Science Foundation of China (grant number: 81600486); Natural Science Foundation of Fujian Province (grant number: 2016J01462, 2018J01314); Young and Middle Aged Talent Training Project of Fujian Provincial Health Commission (grant number: 2018-ZQN-38); the Key Clinical Specialty Discipline Construction Program of Fujian, China (grant number: Min Wei Ke Jiao 2012 No.149); Joint Funds for the innovation of science and Technology, Fujian province (grant number: 2017Y9048, 2019Y9064); and Startup Fund for scientific research, Fujian Medical University (grant number: 2019QH1041).

#### ORCID IDS

Qilan Guo  <https://orcid.org/0000-0002-9000-5643>

Yuehong Huang  <https://orcid.org/0000-0001-7134-719X>

#### REFERENCES

- Kisseleva T, Cong M, Paik Y, Scholten D, Jiang CY, Benner C, Iwaisako K, Moore-Morris T, Scott B, Tsukamoto H, Evans SM, Dillmann W, Glass CK, Brenner DA. Myofibroblasts revert to an inactive phenotype during regression of liver fibrosis. *Proc Natl Acad Sci U S A* 2012;109:9448–53
- Zhang X, Han X, Yin L, Xu L, Qi Y, Xu Y, Sun H, Lin Y, Liu K, Peng J. Potent effects of dioscin against liver fibrosis. *Sci Rep* 2015;5:9713
- Gur C, Doron S, Kfir-Erenfeld S, Horwitz E, Abu-Tair L, Safadi R, Mandelboim O. NKp46-mediated killing of human and mouse hepatic stellate cells attenuates liver fibrosis. *Gut* 2012;61:885–93
- Kong D, Zhang F, Zhang Z, Zhang S. Clearance of activated stellate cells for hepatic fibrosis regression: molecular basis and translational potential. *Biomed Pharmacother* 2013;67:246–50
- Jin H, Jia Y, Yao Z, Huang J, Hao M, Yao S, Lian N, Zhang F, Zhang C, Chen X, Bian M, Shao J, Wu L, Chen A, Zheng S. Hepatic stellate cell interferes with NK cell regulation of fibrogenesis via curcumin induced senescence of hepatic stellate cell. *Cell Signal* 2017;33:79–85
- Krizhanovsky V, Yon M, Dickins RA, Hearn S, Simon J, Miething C, Yee H, Zender L, Lowe SW. Senescence of activated stellate cells limits liver fibrosis. *Cell* 2008;134:657–67
- Handayaniingsih AE, Takahashi M, Fukuoka H, Iguchi G, Nishizawa H, Yamamoto M, Suda K, Takahashi Y. IGF-1 enhances cellular senescence via the reactive oxygen species-p53 pathway. *Biochem Biophys Res Commun* 2012;425:478–84
- Nishizawa H, Iguchi G, Fukuoka H, Takahashi M, Suda K, Bando H, Matsumoto R, Yoshida K, Odake Y, Ogawa W, Takahashi Y. IGF-1 induces senescence of hepatic stellate cells and limits fibrosis in a p53-dependent manner. *Sci Rep* 2016;6:34605
- Campisi J. Aging, cellular senescence, and cancer. *Annu Rev Physiol* 2013;75:685–705
- Muñoz-Espín D, Serrano M. Cellular senescence: from physiology to pathology. *Nat Rev Mol Cell Biol* 2014;15:482–96
- Narita M, Núñez S, Heard E, Narita M, Lin AW, Hearn SA, Spector DL, Hannon GJ, Lowe SW. Rb-mediated heterochromatin formation and silencing of E2F target genes during cellular senescence. *Cell* 2003;113:703–16
- Zhang R, Poustovoitov MV, Ye X, Santos HA, Chen W, Daganzo SM, Erzberger JP, Serebriiskii IG, Canutescu AA, Dunbrack RL, Pehrson JR, Berger JM, Kaufman PD, Adams PD. Formation of MacroH2A-containing senescence-associated heterochromatin foci and senescence driven by ASF1a and HIRA. *Dev Cell* 2005;8:19–30
- Narita M, Narita M, Krizhanovsky V, Núñez S, Chicas A, Hearn SA, Myers MP, Lowe SW. A novel role for high-mobility group proteins in cellular senescence and heterochromatin formation. *Cell* 2006;126:503–14
- Nacarelli T, Lau L, Fukumoto T, Zundell J, Fatkhutdinov N, Wu S, Aird KM, Iwasaki O, Kossenkov AV, Schultz D, Noma KI, Baur JA, Schug Z,

- Tang HY, Speicher DW, David G, Zhang R. NAD<sup>+</sup> metabolism governs the proinflammatory senescence-associated secretome. *Nat Cell Biol* 2019;**21**:397–407
15. Verma SK, Garikipati VNS, Krishnamurthy P, Schumacher SM, Grisanti LM, Cimini M, Cheng Z, Khan M, Yue Y, Benedict C, Truongcao MM, Rabinowitz JE, Goukassian DA, Tilley D, Koch WJ, Kishore R. Interleukin-10 inhibits bone marrow fibroblast progenitor Cell-Mediated cardiac fibrosis in Pressure-Overloaded myocardium. *Circulation* 2017;**136**:940–53
  16. Kurosaki F, Uchibori R, Sehara Y, Saga Y, Urabe M, Mizukami H, Hagiwara K, Kume A. AAV6-mediated IL-10 expression in the lung ameliorates Bleomycin-Induced pulmonary fibrosis in mice. *Hum Gene Ther* 2018;**29**:1242–51
  17. Shamskhov EA, Kratochvil MJ, Orcholski ME, Nagy N, Kaber G, Steen E, Balaji S, Yuan K, Keswani S, Danielson B, Gao M, Medina C, Nathan A, Chakraborty A, Bollyky PL, De Jesus Perez VA. Hydrogel-based delivery of IL-10 improves treatment of bleomycin-induced lung fibrosis in mice. *Biomaterials* 2019;**203**:52–62
  18. Huang YH, Shi MN, Zheng WD, Zhang LJ, Chen ZX, Wang XZ. Therapeutic effect of interleukin-10 on CCl4-induced hepatic fibrosis in rats. *World J Gastroenterol* 2006;**12**:1386–91
  19. Huang YH, Chen YX, Zhang LJ, Chen ZX, Wang XZ. Hydrodynamics-based transfection of rat interleukin-10 gene attenuates porcine serum-induced liver fibrosis in rats by inhibiting the activation of hepatic stellate cells. *Int J Mol Med* 2014;**34**:677–86
  20. Huang YH, Chen MH, Guo QL, Chen YX, Zhang LJ, Chen ZX, Wang XZ. Interleukin-10 promotes primary rat hepatic stellate cell senescence by upregulating the expression levels of p53 and p21. *Mol Med Rep* 2018;**17**:5700–7
  21. Huang YH, Chen MH, Guo QL, Chen ZX, Chen QD, Wang XZ. Interleukin-10 induces senescence of activated hepatic stellate cells via STAT3-p53 pathway to attenuate liver fibrosis. *Cell Signal* 2020;**66**:109445
  22. Li T, Kon N, Jiang L, Tan M, Ludwig T, Zhao Y, Baer R, Gu W. Tumor suppression in the absence of p53-mediated cell-cycle arrest, apoptosis, and senescence. *Cell* 2012;**149**:1269–83
  23. Ishak K, Baptista A, Bianchi L, Callea F, De Groote J, Gudat F, Denk H, Desmet V, Korb G, MacSween RN, Phillips MJ, Portmann BG, Poulsen H, Scheuer PJ, Schmid M, Thaler H. Histological grading and staging of chronic hepatitis. *J Hepatol* 1995;**22**:696–9
  24. Chen Z, Trotman LC, Shaffer D, Lin HK, Dotan ZA, Niki M, Koutcher JA, Scher HI, Ludwig T, Gerald W, Cordon-Cardo C, Pandolfi PP. Crucial role of p53-dependent cellular senescence in suppression of pten-deficient tumorigenesis. *Nature* 2005;**436**:725–30
  25. Louis H, Van Laethem JL, Wu W, Quertinmont E, Degraef C, Van den Berg K, Demols A, Goldman M, Le Moine O, Geerts A, Devière J. Interleukin-10 controls neutrophilic infiltration, hepatocyte proliferation, and liver fibrosis induced by carbon tetrachloride in mice. *Hepatology* 1998;**28**:1607–15
  26. Hung KS, Lee TH, Chou WY, Wu CL, Cho CL, Lu CN, Jawan B, Wang CH. Interleukin-10 gene therapy reverses thioacetamide-induced liver fibrosis in mice. *Biochem Biophys Res Commun* 2005;**336**:324–31
  27. Kong X, Feng D, Wang H, Hong F, Bertola A, Wang FS, Gao B. Interleukin-22 induces hepatic stellate cell senescence and restricts liver fibrosis in mice. *Hepatology* 2012;**56**:1150–9
  28. Mitra A, Satelli A, Yan J, Xueqing X, Gagea M, Hunter CA, Mishra L, Li S. IL-30 (IL27p28) attenuates liver fibrosis through inducing NKG2D-*rae1* interaction between NKT and activated hepatic stellate cells in mice. *Hepatology* 2014;**60**:2027–39
  29. Jin H, Lian N, Zhang F, Chen L, Chen Q, Lu C, Bian M, Shao J, Wu L, Zheng S. Activation of PPAR $\gamma$ /P53 signaling is required for curcumin to induce hepatic stellate cell senescence. *Cell Death Dis* 2016;**7**:e2189
  30. Jin H, Lian N, Zhang F, Bian M, Chen X, Zhang C, Jia Y, Lu C, Hao M, Yao S, Shao J, Wu L, Chen A, Zheng S. Inhibition of Yap signaling contributes to senescence of hepatic stellate cells induced by tetramethylpyrazine. *Eur J Pharm Sci* 2017;**96**:323–33
  31. Li P, Gan Y, Xu Y, Song L, Wang L, Ouyang B, Zhang C, Zhou Q. The inflammatory cytokine TNF- $\alpha$  promotes the premature senescence of rat nucleus pulposus cells via the PI3K/akt signaling pathway. *Sci Rep* 2017;**7**:42938
  32. Ruigrok MJR, Xian JL, Frijlink HW, Melgert BN, Hinrichs WLJ, Olinga P. siRNA-mediated protein knockdown in precision-cut lung slices. *Eur J Pharm Biopharm* 2018;**133**:339–48

(Received July 3, 2020, Accepted August 28, 2020)